



Journal of
**Pharmacology and
Toxicology**

ISSN 1816-496X



Academic
Journals Inc.

www.academicjournals.com

Molecular Modelling Analysis of the Metabolism of Fentanyl

Fazlul Huq

School of Biomedical Sciences,

Faculty of Health Sciences, C42, The University of Sydney,

P.O. Box 170, Lidcombe, NSW 1825, Australia

Abstract: Fentanyl (FT) is a synthetic μ -opioid receptor agonist, widely used for surgical analgesia and sedation. FT undergoes rapid and extensive hepatic biotransformation to metabolites that result from hydrolysis, N-delalkylation and hydroxylation reactions. The major metabolite is norfentanyl (NFT) formed from N-delalkylation. CYP3A4 is responsible for the oxidative dealkylation of FT in the human liver suggesting that FT may be subject to drug interactions in vivo as numerous other therapeutic agents including nifedipine, lidocaine and paracetamol are metabolized by the same enzyme. The toxicity of FT may be in part due to CYP3A4*1B and CYP3A5*3 variant alleles, resulting into variation in FT metabolism. Molecular modelling analyses based on molecular mechanics, semi-empirical (PM3) and DFT (at B3LYP/6-31G* level) calculations show that FT and all its metabolites have large LUMO-HOMO energy differences so that they would be kinetically inert. However, the molecular surfaces of FT, PAL and NFT are found to abound in electron-deficient regions so that they may be subject to nucleophilic attack by glutathione and nucleobases in DNA resulting into glutathione depletion and DNA damage, respectively. The kinetic inertness of the molecules means that the rates of such adverse reactions would be low unless the reactions are speeded up enzymatically.

Key words: Fentanyl, analgesic, surgery, synthetic μ -opioid, norfentanyl, molecular modelling

INTRODUCTION

Fentanyl (FT, N-phenyl-N-(1-(2-phenylethyl)-4-piperidiny)-propanamide) is a synthetic μ -opioid receptor agonist, widely used for surgical analgesia and sedation (Hug and Murphy, 1981). It is the preferred induction and maintenance anaesthetic agent in cardiac surgery, having had short analgesic effect and relatively short duration of action (Mather, 1983). FT was introduced into clinical use in the 1960s. FT has been reported to be 5-100 times more potent than morphine (Van Nimmen *et al.*, 2004).

FT undergoes rapid and extensive hepatic biotransformation to metabolites that result from hydrolysis, N-delalkylation and hydroxylation reactions. Intestinal microsomes are also found to metabolize FT. The major metabolite norfentanyl (NFT) is formed from N-delalkylation. CYP3A4 is responsible for the oxidative dealkylation of FT in the human liver (Guitton *et al.*, 1997), suggesting that FT may be subject to drug interactions in vivo as numerous other therapeutic agents including nifedipine, lidocaine and paracetamol are metabolized by the same enzyme (Freeman, 2000). The toxicity of FT may be in part due to CYP3A4*1B and CYP3A5*3 variant alleles, resulting into variant FT metabolism (Ming *et al.*, 2005).

In this study molecular modelling analyses have been carried out for FT and its metabolites in order to obtain a better understanding of toxicity due to FT and its metabolites. The study was carried out in the School of Biomedical Sciences, The University of Sydney during February to July 2006.

COMPUTATIONAL METHODS

The geometries of FT and the metabolites NFT, PAL, PAA and 2PE have been optimised based on molecular mechanics (Fig. 1), semi-empirical and DFT calculations, using the molecular modelling program Spartan 02. Molecular mechanics calculations were carried out using MMFF force field. Semi-empirical calculations were carried out using the routine PM3. DFT calculations were carried out using the program Spartan 02 (Spartan, 2002) at B3LYP/6-31G* level. In optimization calculations, a RMS gradient of 0.001 was set as the terminating condition. For the optimised structures, single point calculations were carried to give heat of formation, enthalpy, entropy, free energy, dipole moment, solvation energy, energies for HOMO and LUMO. The order of calculations: molecular mechanics followed by semi-empirical followed by DFT ensured that the structure was not embedded in a local minimum. To further check whether the global minimum was reached, some calculations were carried out with improvable structures. It was found that when the stated order was followed, structure corresponding to the global minimum or close to that could ultimately be reached in all cases. Although RMS gradient of 0.001 may not be sufficiently low for vibrational analysis, it is believed to be sufficient for calculations associated with electronic energy levels.

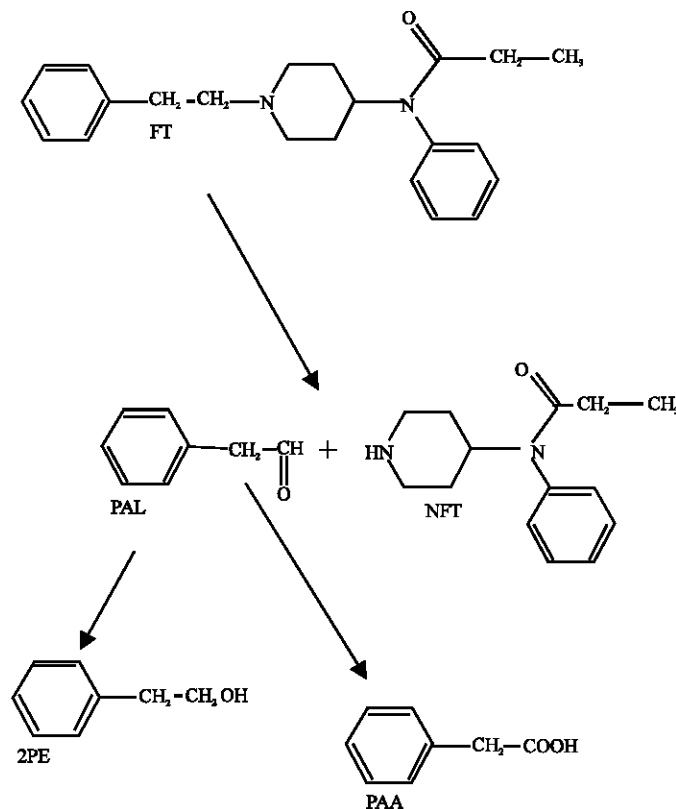


Fig. 1: Metabolic pathways of fentanyl (Based on Tateishi *et al.*, 1995)

RESULTS AND DISCUSSION

Table 1 gives the total energy, heat of formation as per PM3 calculation, enthalpy, entropy, free energy, surface area, volume, dipole moment, energies of HOMO and LUMO as per both PM3 and DFT calculations for FT and their metabolites NFT, PAL, PAA and 2PE. Figure 2-6 give the regions of negative electrostatic potential (greyish-white envelopes) in (a), HOMOs (where red indicates HOMOs with high electron density) in (b), LUMOs in (c) and density of electrostatic potential on the molecular surface (where red indicates negative, blue indicates positive and green indicates neutral) in (d) as applied to the optimised structures of FT, NFT, PAL, PAA and 2PE. The calculated solvation energies of FT, NFT, PAL, PAA and 2PE from PM3 calculations in kcal mol⁻¹ are, respectively -5.74, -8.70, -4.63, -10.73 and -6.10 and their dipole moments from DFT calculations are 3.8, 4.3, 2.7, 4.9 and 1.5, respectively. The results suggest that PAA would be most soluble in water whereas FT (with the possible exception of PAL) would have the lowest solubility in water.

The calculated LUMO-HOMO energy differences for FT, NFT, PAL, PAA and 2PE are found to be large (that ranges from 5.75 to 6.50 eV from DFT calculations), indicating that the compounds would all be kinetically inert. 2PE is expected to be most inert whereas PAL is expected to be least inert.

The molecular surface of FT, NFT, PAL and PAA are found to abound in positive (blue) regions, indicating the compounds are more likely subject to nucleophilic attack such as that by glutathione and nucleobases in DNA. Reaction with glutathione would cause glutathione depletion and hence cellular toxicity whereas oxidation of nucleobases in DNA would cause DNA damage.

When the surface area and volume of FT are compared with those of NFT, PAL, PAA and 2PE, it is found that the values for FT are distinctly different from those of the metabolites, indicating that none of the metabolites is likely to be a substrate for the enzyme to which FT binds.

In the case of FT, NFT and PAL, the electrostatic potential is found to be more negative around the carbonyl oxygen atom, indicating that the position may be subject to electrophilic attack. In the

Table 1: Calculated thermodynamic and other parameters of fentanyl and its metabolites

Moldecue	Calculation type	Total energy (kcal mol ⁻¹ / atomic unit*)	Heat of formation (kcal mol ⁻¹)	Enthalpy (kcal mol ⁻¹)	Entropy (cal mol ⁻¹)	Solvation energy (kcal mol ⁻¹)
FT	PM3	-13.91	-8.17	298.92	161.53	-5.74
	DFT	-1039.74		299.97	160.24	-4.67
NFT	PM3	-36.55	-27.84	209.37	123.91	-8.70
	DFT	-730.26		210.46	122.88	-7.66
PAL	PM3	-20.29	-15.67	90.48	87.15	-4.63
	DFT	-384.88		91.66	90.17	-3.64
PAA	PM3	-82.02	-71.29	95.23	91.11	-10.73
	DFT	-460.14		95.73	94.40	-6.79
2PE	PM3	-37.03	-30.94	105.58	90.77	-6.10
	DFT	-386.09		107.12	90.93	-5.99

Moldecue	Calculation type	Feer enger (kcal mol ⁻¹)	Area (Å ²)	Volume (Å ³)	Dipole moment (debye)	HOMO (ev)	LUMO (ev)	LUMO- HOMO (ev)
FT	PM3	250.76	393.75	381.76	3.6	-9.33	0.21	9.54
	DFT	252.22	400.52	382.82	3.8	-6.02	-0.06	5.96
NFT	PM3	172.43	273.24	260.19	3.6	-9.33	0.25	9.58
	DFT	173.84	278.55	260.98	4.3	-6.05	-0.05	6.00
PAL	PM3	64.49	155.64	137.81	2.5	-9.73	0.07	9.80
	DFT	64.77	158.08	138.76	2.7	-6.59	-0.84	5.75
PAA	PM3	68.07	162.59	144.56	4.5	-10.03	-0.25	9.78
	DFT	67.58	164.06	145.13	4.9	-6.87	-0.66	6.21
2PE	PM3	78.52	164.02	142.95	1.4	-9.63	0.23	9.86
	DFT	80.01	164.95	143.56	1.5	-6.50	-0.00	6.50

* in atomic units from DFT calculations

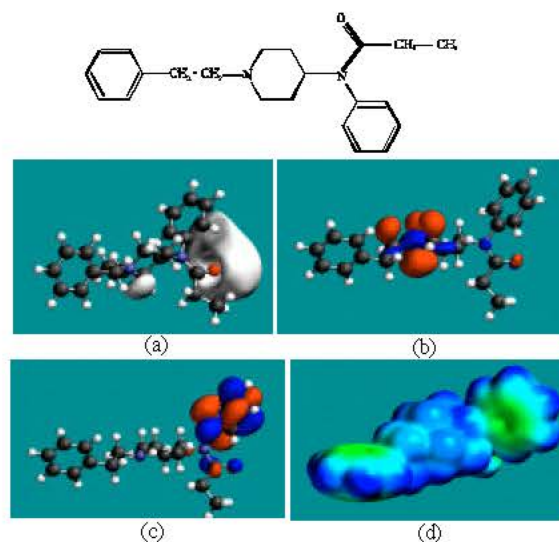


Fig. 2: Structure of FT giving in: (a) the electrostatic potential (greyish envelope denotes negative electrostatic potential), (b) the HOMOs, (where red indicates HOMOs with high electron density) (c) the LUMOs (where blue indicates LUMOs) and in (d) surface electric charges (where red indicates negative, blue indicates positive and green indicates neutral)

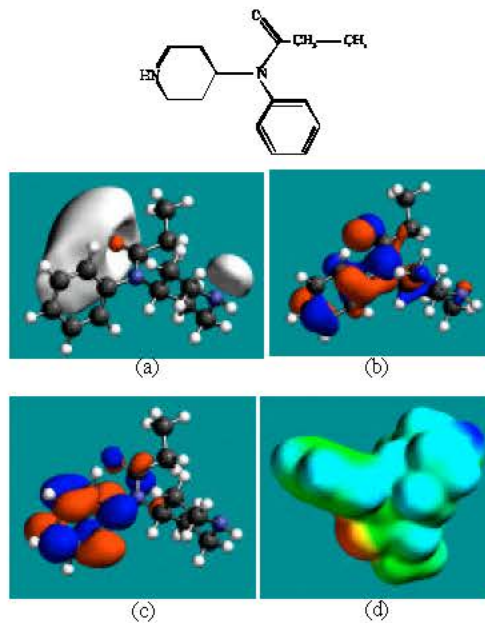


Fig. 3: Structure of NFT giving in: (a) the electrostatic potential (greyish envelope denotes negative electrostatic potential), (b) the HOMOs, (where red indicates HOMOs with high electron density) (c) the LUMOs (where blue indicates LUMOs) and in (d) surface electric charges (where red indicates negative, blue indicates positive and green indicates neutral)

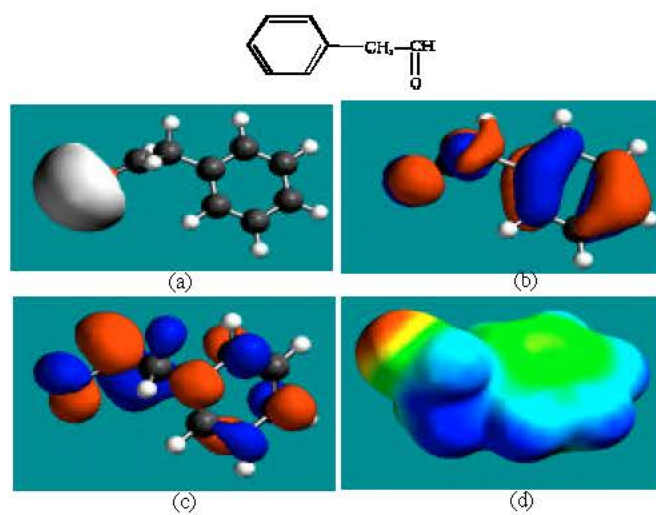


Fig. 4: Structure of PAL giving in: (a) the electrostatic potential (greyish envelope denotes negative electrostatic potential), (b) the HOMOs, where red indicates HOMOs with high electron density (c) the LUMOs (where blue indicates LUMOs) and in (d) surface electric charges (where red indicates negative, blue indicates positive and green indicates neutral)

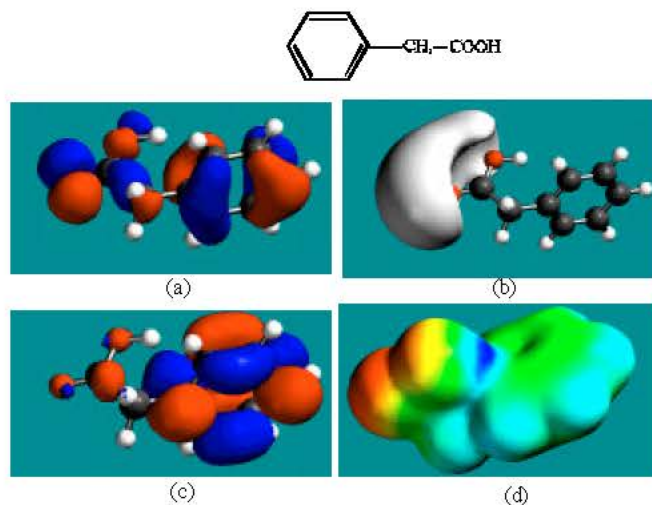


Fig. 5: Structure of PAA giving in: (a) the electrostatic potential (greyish envelope denotes negative electrostatic potential), (b) the HOMOs, (where red indicates HOMOs with high electron density) (c) the LUMOs (where blue indicates LUMOs) and in (d) surface electric charges (where red indicates negative, blue indicates positive and green indicates neutral)

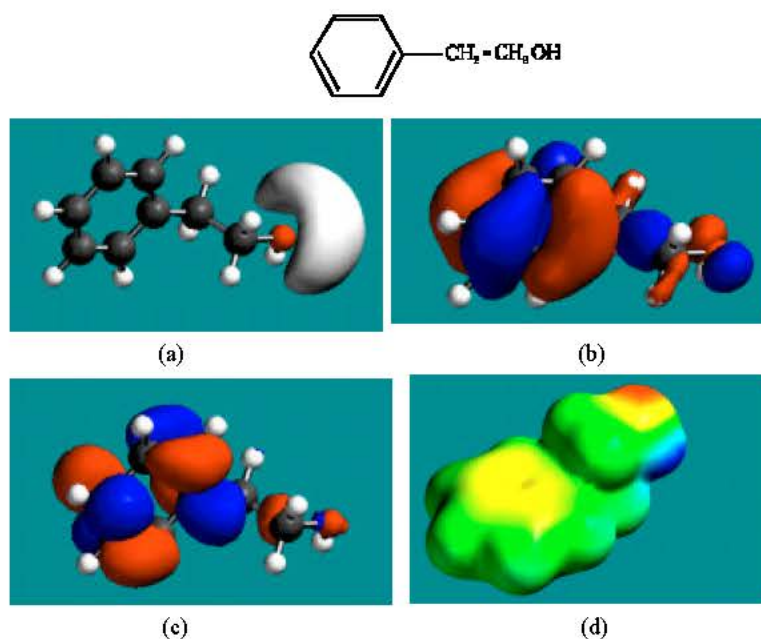


Fig. 6: Structure of 2PE giving in: (a) the electrostatic potential (greyish envelope denotes negative electrostatic potential), (b) the HOMOs, (where red indicates HOMOs with high electron density) (c) the LUMOs (where blue indicates LUMOs) and in (d) surface electric charges (where red indicates negative, blue indicates positive and green indicates neutral)

case of PAA, the electrostatic potential is found to be more negative around the carbonyl and hydroxyl oxygen atoms, indicating that the positions may be subject to electrophilic attack. In the case of 2PE, the electrostatic potential is found to be more negative around the hydroxyl oxygen atom, indicating once again that the position may be subject to electrophilic attack.

In the case of FT, the HOMOs with high electron density are found close to the non-hydrogen atoms of the piperidinyl ring whereas the LUMOs are found close to the non-hydrogen atoms of the phenyl ring that is bonded to the tertiary nitrogen atom. In the case of NFT, both the HOMOs with high electron density and the LUMOs are found close to the non-hydrogen atoms of the phenyl ring. In the case of PAL, both the HOMOs with high electron density and the LUMOs are found close to all the non-hydrogen atoms. In the case of PAA and 2PE also, both the HOMOs with high electron density and the LUMOs are found close to most of the non-hydrogen atoms.

CONCLUSIONS

Molecular modelling analyses based on semi-empirical and DFT calculations show that FT, NFT, PAL, PAA and 2PE all have large LUMO-HOMO energy differences so that they would be kinetically inert. The molecular surfaces of FT, NFT and PAL are found to abound in electron-deficient regions so that they may be subject to nucleophilic attack by glutathione and nucleobases in DNA, resulting into glutathione (and hence cellular toxicity) and DNA damage, respectively. However, the kinetic inertness of the molecules means that the rates of such adverse reactions would be low unless the reactions are speeded up enzymatically.

ABBREVIATIONS

FT: Fentanyl; N-phenyl-N-(1-(2-phenylethyl)-4-piperidinyl)-propanamide
NFT: Norfentanyl
DFT: Density functional theory
LUMO: Lowest unoccupied molecular orbital
HOMO: Highest occupied molecular orbital

ACKNOWLEDGMENTS

Fazlul Huq is grateful to the School of Biomedical Sciences, The University of Sydney for the time release from teaching.

REFERENCES

- Freeman, D.E., 2000. The effect of paracetamol (acetaminophen) on fentanyl metabolism *in vivo*. *Acta Anaesthesiol. Scand.*, 44: 560-563.
- Guitton, J., T. Buronfosse, M. Desage, A. Lapape, J.-L. Brazier and P. Beaune, 1997. Possible involvement of multiple cytochrome P450s in Fentanyl and Sufentanil metabolism as opposed to Alfentanil. *Biochem. Pharmacol.*, 53: 1613-1619.
- Hug, C.C. and M.R. Murphy, 1981. *Anaesthesiology*, 55: 369.
- Mather, L.E., 1983. Clinical pharmacokinetics of fentanyl and its newer derivatives, *Clin. Pharmacokinet.*, 8: 422-446.
- Ming, J., S.B. Gock, P.J. Jannetto, J.M. Jentzen and S.H. Wong, 2005. Pharmacogenomics as molecular autopsy for forensic toxicology: Genotyping cytochrome P450 3A4*1B and 3A5*3 for 25 fentanyl cases, *J. Analyt. Toxicol.*, 29: 590-598.
- Spartan, 2002., Wavefunction, Inc. Irvine, CA, USA, 2002.
- Tateishi, T., A.I.J. Wood, F.P. Guengerich and M. Wood, Biotransformation of tritiated fentanyl in human liver microsomes. *Biochem. Pharmacol.*, 50: 1921-1924.
- Van Nimmen, N.F.J., K.L.C. Poels and H.A.F. Veulemans, 2004. Highly sensitive gas chromatographic-mass spectrometric screening method for the determination of pictogram levels of fentanyl, sufentanil and alfentanil and their major metabolites in urine of opioid exposed workers. *J. Chromatogr. B*, 804: 375-387.